Microvolume field-effect *p*H sensor for the scanning probe microscope

S. R. Manalis[a] and E. B. Cooper
Media Laboratory, Massachusetts Institute of Technology, Cambridge, Massachusetts 02139

P. F. Indermuhle, P. Kernen, and P. Wagner
Zyomyx, 3911 Trust Way, Hayward, California 94545

D. G. Hafeman
Molecular Devices, 1311 Orleans Drive, Sunnyvale, California 94089

S. C. Minne and C. F. Quate
E. L. Ginzton Laboratory, Stanford University, Stanford, California 94305-4085

(Received 23 November 1999; accepted for publication 15 December 1999)

A *p*H sensitive scanning probe is realized by integrating a micron-sized field-effect sensor onto a cantilever designed for an atomic force microscope. The hybrid device, called a scanning probe potentiometer (SPP), is capable of measuring *p*H gradients over a sample surface. The device was used to profile the *p*H across a reservoir of laminar streams created by fluid flow in an array of microfluidic channels of varying *p*H. When a single SPP scanned, a 1.5 mm reservoir in a 10-channel array, the *p*H profile was measured in less than 1 min with a spatial resolution of 10 μm and sensitivity of less than 0.01 *p*H units. © *2000 American Institute of Physics.* [S0003-6951(00)01307-3]

A growing trend in biotechnology and medical diagnostics is to increase speed and sensitivity of analysis while reducing reagent cost by reducing reagent volume. Much of the progress in this direction is catalyzed by the ability to organize high-density arrays of DNA, proteins, or cells on a surface coupled with technology for building functional devices on the micron and nanometer scale. There is also a desire to analyze or ''read'' such molecular arrays without the need to label the molecules with chromophores, fluorophores, or enzymes to enable optical detection.

Nonoptical tools available include the atomic force microscope (AFM)[1] and electrochemical and field-effect devices, such as the ion sensitive field-effect transistor (ISFET)[2] and the light addressable potentiometric sensor (LAPS).[3] The AFM allows high force sensitivity mapping of biological cells and molecules such as DNA and proteins.[4] The AFM can obtain stable images of individual biomolecules while operating in physiological environments. An advantage of the AFM over optical detection is that molecules can be imaged directly, and the dimensions of the probe determine the spatial resolution. When equipped with special probes, such as chemically modified nanotubes[5] or silica spheres,[6] the AFM is capable of detecting the molecular charge.

The benefit of the field-effect device is that it can directly detect molecular and ionic charge. The LAPS device has been used in a microphysiometer to monitor the response of cells to chemical substances by measuring the rate of change of *p*H as protons are excreted from the cells during metabolism.[7] In other work, a silicon field-effect device was used to measure the *in situ* hybridization of unlabeled DNA.[8] This experiment is a powerful demonstration of how electronic detection can eliminate the inconvenient and costly process of labeling DNA probes with fluorescent or radiochemical tags. Although the active area of most field-effect sensors is greater than a square millimeter, scaling the devices shows promise towards improving spatial resolution and charge sensitivity.[9]

Here, we describe a new system for sensing molecular and ionic charge that incorporates key elements of the field-effect sensor and the atomic force microscope. We have combined these systems by integrating a $10\,\mu\text{m}\times 10\,\mu\text{m}\times 20\,\mu$mLAPS on a cantilever designed for the atomic force microscope. When compared to the conventional LAPS,[3,7] the active area is reduced by 10^4 and the total silicon volume is reduced by over 10^6. The hybrid device, called the scanning probe potentiometer (SPP), has the ability to profile *p*H changes on the surface of an arbitrary sample. The SPP is also capable of imaging the topography of a sample when operated with the AFM.

We show that the SPP is capable of profiling the *p*H distribution of a patterned array of fluidic streams. Multiple solutions are organized on a surface with an open array of microfluidic channels. The multiplicity of channels converges at a single junction, and because the flow within the channels is laminar at the junction, the solutions do not mix. The *p*H in the multiplicity of channels can be monitored in real time by scanning a single SPP across the junction. In this manner, we have analyzed up to ten different solutions (from ten different channels) in less than one minute while consuming 500 nl of each solution. The sensitivity of the SPP is less than 0.01 *p*H units and the spatial resolution is 10 μm. Together, the SPP and the microfluidic array provide a scalable approach for high throughput, low volume *p*H analysis.

The SPP incorporates a silicon LAPS structure at the end of a silicon nitride cantilever and is microfabricated using conventional photolithography. A cross-sectional schematic

[a]Electronic mail: scottm@media.mit.edu

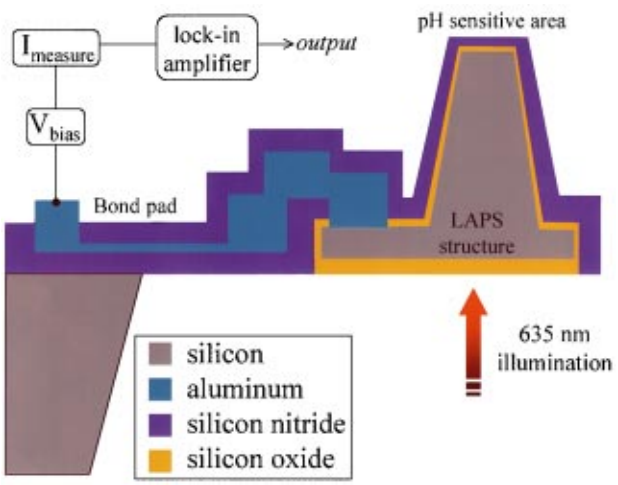

FIG. 1. (Color) Cross-sectional schematic of the scanning probe potentiometer (SPP).

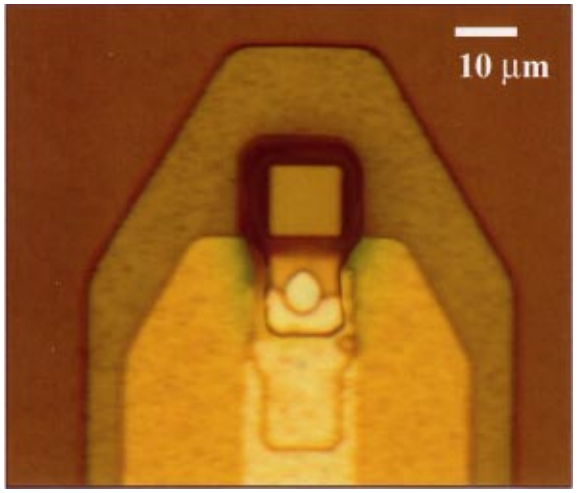

FIG. 2. (Color) Optical micrograph of the silicon LAPS structure integrated on a silicon nitride cantilever that is ~1.3 μm thick and 350 μm long. The *p*H sensitive area of this device is 100 μm^2 and protrudes approximately 10 μm above the nitride cantilever. Since the topography is much larger than the optical depth of focus, the image was computer generated by superimposing three images acquired at three optical focal lengths. Electrical connection is made to the LAPS structure through a bond pad located on the cantilever die.

of the SPP is shown in Fig. 1. The fabrication process begins by using an anisotropic etch to pattern the LAPS in the top layer of a silicon-on-insulator wafer (10 μm silicon on 2250 Å buried oxide). This etch is stopped by the buried oxide layer which is subsequently removed with buffered hydrofluoric acid. The LAPS structure is passivated with 6000 Å of low-pressure chemical vapor deposition (LPCVD) nitride on 500 Å of thermal oxide. Both films are removed from the apex surface of the LAPS with an anisotropic dry etch, while the substrate nitride is protected with ~1 μm of photoresist. The etch removes all of the nitride from the apex while the nitride on the vertical sidewalls remains. The *p*H sensitive area is formed on the apex by depositing an additional 600 Å of LPCVD nitride on 300 Å thermal oxide. Contact holes are then etched at the base of the nitride-coated LAPS structure and 1 μm of Al is patterned over the contact area and also at the bonding area that is located a few millimeters away from the LAPS. In order to reduce the stress in the cantilever, the contact area is connected to the bonding area with a thin, 700 Å layer of Al. The Al is passivated with 6000 Å of plasma enhanced CVD (PECVD) nitride that is deposited on 1000 Å of low-temperature silicon oxide. The nitride is removed again from the *p*H sensitive area and also over the bonding area. The cantilevers are released by protecting the front of the wafer with polyimide while etching the back in EDP for ~8 h at 105 °C. The polyimide is removed with an O_2 plasma etch. An optical micrograph of the final device is shown in Fig. 2.

A custom fluidic delivery system consisting of a 10-channel array was used to demonstrate the capability of the prototype SPP. An optical micrograph of a 10-channel array is shown in Fig. 3. The channels are defined in silicon with a deep reactive ion etch and are patterned to intersect into a common reservoir. A top view of this reservoir is shown in Fig. 3(a). In this image, the microscope is focused on the top of the channels (colored region) and the dark areas are shadows from the bottom of the channels. The channel depth is ~200 μm and is revealed in the cross-sectional image shown in Fig. 3(b). Because the channel volume is low, the Reynolds number is sufficiently low to maintain laminar flow for reasonable flow rates. The concept of laminar flow within intersecting junctions has been demonstrated previously.[10] With laminar flow, the solutions emanating from the ten channels do not mix in the reservoir. The solution flow rate is set to a maximum value 500 nl/min for a channel width of 110 μm. If the flow rate is further increased, the solution will leak out of the channels. By increasing the channel spacing to 200 μm, the flow rate can be increased to over 10 μl/min.

The operating principle of the LAPS has been described in previous work[3,7] and is only summarized here. The LAPS is connected to an external circuit that is used to measure both an alternating photocurrent and to apply a bias voltage between the silicon and electrolyte solution. The photocurrent is generated by illuminating the silicon with an intensity

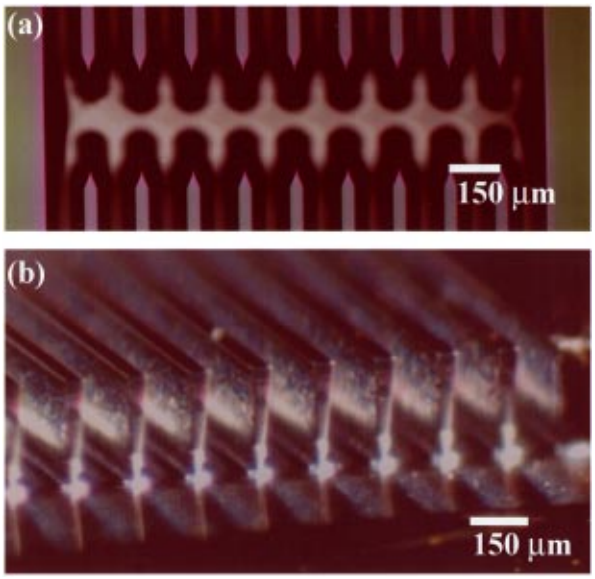

FIG. 3. (Color) (a) Top view of the microfluidic channel array. The channels are defined in silicon with a deep reactive ion etch (DRIE) to a depth of ~200 μm. (b) Cross section of channel array. Solutions are pumped through the open channel array with a syringe pump that holds ten syringes.

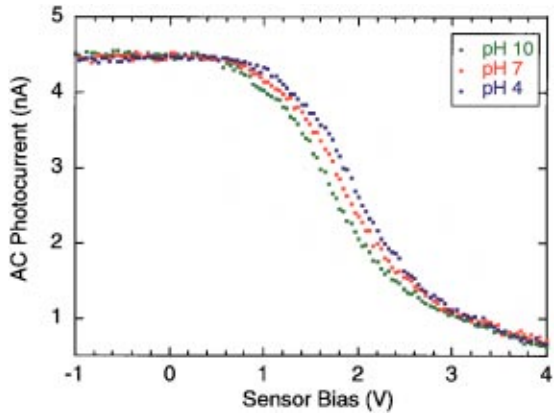

FIG. 4. (Color) Alternating photocurrent vs applied bias voltage (V) between the LAPS and electrolyte solution. The curve is measured in three channels that contain a buffer solution of pH 4, 7, 10. The LAPS measurement is made with p-type silicon with a doping of $\sim 10^{14}$ cm^{-3}. The solution is grounded downstream of the reservoir with an aluminum electrode. A 635 nm laser diode is intensity modulated (near 100%) at a frequency of 7 kHz and a lock-in amplifier is used to measure the alternating photocurrent amplitude. The pH sensitivity of the present LAPS devices ranged from 40 to 50 mV per pH unit, which is slightly below the expected value of 61 mV/unit at 23 °C. For solutions of similar ionic conductivity, pH can be determined by measuring I, while fixing the bias at the maximum I vs V slope. Since the width of the $I-V$ transition is nearly 2 V, the pH response is fairly linear over a wide pH range. The described measurement can be calibrated to the sensor potential provided the $I-V$ slope is known. The rms noise of the LAPS is less than 500 μV which yields a pH sensitivity of $\sim$0.01 units.

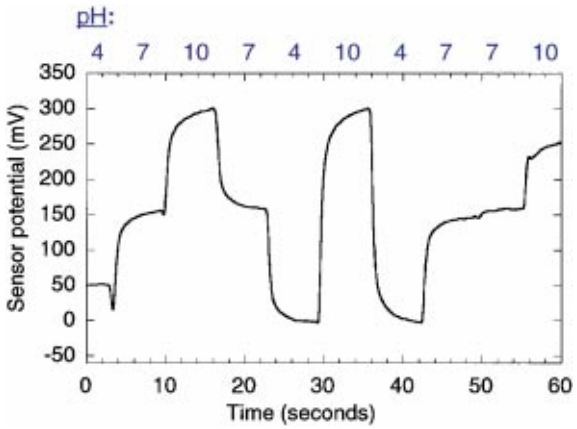

FIG. 5. (Color) Surface potential of the LAPS vs time as the SPP is scanned across the junction shown in Fig. 3(a). The cantilever stops in each channel for a period of 5 s. The pH of the buffer solution in each channel is listed above the plot. The channel pitch is 150 μm and the flow rate is 500 nl/min.

modulated laser diode. Between the electrolyte and silicon is a thin layer of silicon nitride. Silicon nitride is sensitive to pH over a wide pH range due to the proton binding capacity of Si–O and $SiNH_2$ groups at the electrolyte interface. The surface potential at this interface is related to the surface density of protons. The electric field in the space-charge region of the silicon adjacent to the sensing surface is dependent upon the sum of the applied bias voltage and the surface potential. When the silicon is forward biased, no photocurrent flows through the external circuit. When the silicon is reversed biased, a depletion region is formed below the region of thin nitride. The voltage gradient in the depletion region separates electron-hole pairs created by the intensity modulated illumination. This creates an alternating photopotential that drives an alternating photocurrent through the external circuit under reverse-bias conditions. Direct current between the silicon and electrolyte is negligible. In Fig. 4, the amplitude of the photocurrent (I) is plotted as a function of applied bias (V) for solution of pH 4, 7, and 10.

The pH from multiple solutions is profiled by scanning the SPP across the reservoir formed at the junction of the ten channels, while carrying out the analysis described in the legend of Fig. 4. A plot of the sensor potential versus time during the scanning process is shown in Fig. 5. The relative potential difference between each channel correlates closely to the actual channel pH (listed above the plot) except for the first and last edge channels. The SPP is scanned with a computer-controlled motor that translates the channel array in steps equal to the channel pitch. The travel time between channels is $\sim$ 1 s, the wait time at a given channel is 5 s, and the flow rate is 500 nl/min. The pH resolution of the LAPS sensors is less than 0.01 pH units in a 1 Hz bandwidth.

In summary, we used a microfabricated cantilever with an integrated field-effect sensor to profile the pH of laminar streams within a microfluidic channel array. The combined system is scalable, and provides a high-resolution tool for directly synthesizing, switching, and investigating nanoliter volumes in a plurality of discrete solutions. We envision that the scanning probe potentiometers can be used to image pH gradients produced by individual cells as well as the charge distribution from patterned arrays of biomolecules such as DNA and proteins.

One of the authors (S.R.M.) acknowledges the support by the MIT Media Lab's Things That Think (TTT) consortium; E.B.C. is supported by a graduate fellowship from Motorola; C.F.Q. acknowledges support by DARPA and ONR.

[1] G. Binnig, C. F. Quate, and Ch. Gerber, Phys. Rev. Lett. **12**, 930 (1986).
[2] P. Bergveld, IEEE Trans. Biomed. Eng. **19**, 342 (1972).
[3] D. G. Hafeman, J. W. Parce, and H. M. McConnell, Science **240**, 1182 (1988).
[4] H. G. Hansma, J. Vesenka, C. Siegerist, G. Kelderman, H. Morrett, R. L. Sinsheimer, V. Elings, C. Bustamante, and P. K. Hansma, Science **256**, 1180 (1992); W. A. Rees, R. W. Keller, J. P. Vesenka, G. Yang, and C. Bustamante, *ibid.* **260**, 1646 (1993)
[5] S. S. Wong, E. Joselevich, A. T. Woolley, C. L. Cheung, and C. M. Lieber, Nature (London) **394**, 52 (1998).
[6] K. Hu, R. Pyati, and A. J. Bard, Anal. Chem. **70**, 2870 (1998).
[7] H. M. McConnell, J. C. Owicki, J. W. Parce, D. L. Miller, G. T. Baxter, H. G. Wada, and S. Pitchford, Science **257**, 1906 (1992); J. W. Parce, J. C. Owicki, K. M. Kercso, G. B. Sigal, H. G. Wada, V. C. Muir, L. J. Bousse, K. L. Ross, B. I. Sikic, and H. M. McConnell, *ibid.* **246**, 243 (1989); J. C. Owicki, L. J. Bousse, D. G. Hafeman, G. L. Kirk, J. D. Olson, H. G. Wada, and J. W. Parce, Annu. Rev. Biophys. Biomol. Struct. **23**, 87 (1994).
[8] E. Souteyrand, J. P. Cloarec, J. R. Martin, C. Wilson, I. Lawrence, S. Mikkelsen, and M. F. Lawrence, J. Phys. Chem. B **101**, 2980 (1997).
[9] Y. Ito, Sens. Actuators B **52**, 107 (1998); M. Nakao, S. Inoue, T. Yoshinobu, and H. Iwasaki, *ibid.* **34**, 234 (1996); S. Inoue, M. Nakao, T. Yoshinobu, and H. Iwasaki, *ibid.* **32**, 23 (1996).
[10] P. J. A. Kenis, R. F. Ismagilov, and G. M. Whitesides, Science **285**, 83 (1999).